

ADHESIVE FORCE OF FLAT INDENTERS WITH BRUSH-STRUCTURE

UDC 539.3

Qiang Li¹, Valentin L. Popov^{1,2,3}

¹Berlin University of Technology, Berlin, Germany

²National Research Tomsk State University, Tomsk, Russia

³National Research Tomsk Polytechnic University, Tomsk, Russia

Abstract. *We have numerically studied adhesive contact between a flat indenter with brush structure and an elastic half space using the boundary element method. Various surface structures with different size, number and shape of the “pillars”, as well as their distributions (regular or random) have been investigated. The results validate the theoretical prediction that the adhesive force in contact of an indenter with discontinuous areas is roughly proportional to the square root of the real contact density (“filling factor”).*

Key Words: *Adhesion, Brush Structure, Filling Factor, Boundary Element Method*

1. INTRODUCTION

Textured surfaces are gaining popularity today due to their special physical properties such as nanotextured surface for improvement of water repellent [1] or bactericidal properties of orthopedic implants [2] or tribological properties in hydrodynamic lubrication [3]. Some of these structure designs try to mimic the “mystical” property of nature. One interesting example is adhesion of the geckos. It was found that there are 6.5 million setae on the gecko’s feet which could provide a large adhesive force [4]. It was argued that this contact splitting is the one that enhances adhesion [5, 6]. In the present paper we consider adhesion between a rigid flat surface with columns and an elastic half space (see Fig.1) under usual assumptions of the JKR-theory (see e.g. [7]).

Received December 20, 2017 / Accepted January 31, 2018

Corresponding author: Qiang, Li

Affiliation: Berlin University of Technology, Sekr. C8-4, Straße des 17. Juni 135, D-10623 Berlin

E-mail: qiang.li@tu-berlin.de

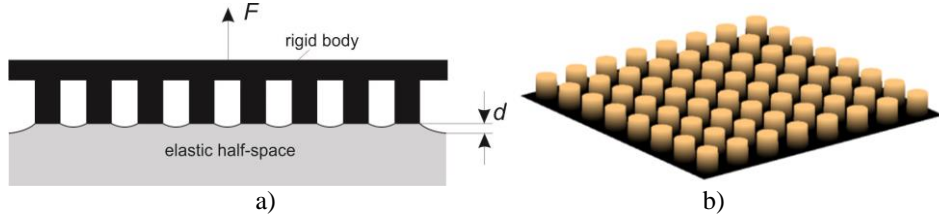


Fig. 1 Contact configuration: a) sketch of adhesive pull-off experiment with contact between a rigid structure and an elastic half-space; b) an example of a brush-structured surface

The classical theory of adhesion between a flat cylindrical punch and an elastic half space was given by Kendall in 1971 [8]. Over the last few years, several analytical models have been proposed to provide for understanding of adhesive behavior of microcontacts of a cluster structure [9-11]. A detailed review can be found in [12]. Three-dimensional numerical methods, in particular the boundary element method have been recently very frequently used to simulate the pull-off process of adhesive contact of different indenters, for example based on the JKR-model (Johnson, Kendall and Roberts) by Pohrt and Popov (2015) [13], or using the Dugdale potential by Bazrafshan et al. (2017) [14], and by Molibari et al. (2017) [15]. In this paper we will use the method of [13] to simulate adhesive contacts of the cluster system. This method can be applied to various adhesive contact problems, while some of them have been validated by existing theories or analytical solutions: the case of a spherical indenter validated by the classical JKR theory [16], the case of a cylindrical punch by Kendall's theory, tests with toroidal indenter, can be found in [17], and with elliptical one as well as two circular punches in [18]. Recently the BEM has been extended for contacts of power-law functionally graded materials [19] and has been validated by the theoretical solution and the method of the dimensionality reduction [20]. This effective numerical tool enables us to carry out simulation of various brush structures.

2. ANALYTICAL ESTIMATION

A recent study of the influence of contact geometry on the strength of adhesion states that the filling factor (or ratio of real area to the apparent area) plays an important role in the adhesive contact of a flat-ended punch with internal discontinuities [21]. If the real contact area of the punch is in proportion to the whole apparent area A with a filling factor ξ , $A_{\text{real}} = \xi A$, then the total energy is equal to

$$U_{\text{tot}} \approx E^* \sqrt{\frac{A}{\pi}} d^2 - \gamma_{12} \xi A \quad (1)$$

where E^* is effective elastic modulus $E^* = E/(1-\nu^2)$ with E the elastic modulus and ν the Poisson's ratio, d is the indentation depth, γ_{12} is the work of adhesion per unit area. The first term in Eq. (1) indicates the elastic energy stored in the body where $(A/\pi)^{1/2}$ represents the "effective radius" of the cross section of the punch, and the second the adhesion energy. The adhesive force and the critical indentation depth can be derived as

$$F_{A,\text{upper}} \approx \sqrt{8\pi E^* \xi \gamma_{12} (A/\pi)^{3/2}}, \quad (2)$$

$$d_{c,\text{upper}} \approx -\sqrt{\frac{2\pi \xi \gamma_{12} \sqrt{A/\pi}}{E^*}}. \quad (3)$$

The subscript ‘‘upper’’ means the upper bound of the force. Similarly, if we use incircle radius a_0 of the apparent area instead of effective radius $(A/\pi)^{1/2}$, then the lower bound of the force and indentation depth is estimated as

$$F_{A,\text{lower}} \approx \sqrt{8\pi E^* \xi \gamma_{12} a_0^3}, \quad (4)$$

$$d_{c,\text{lower}} \approx -\sqrt{\frac{2\pi \xi \gamma_{12} a_0}{E^*}}. \quad (5)$$

Both estimations (2) and (4) show that the adhesive force of discontinuous or structured punch is roughly proportional to the square root of the area of the real contact (and thus square root of the filling factor: $F_A \sim \xi^{1/2}$). Note that we study the indentation depth-controlled pull off experiment, and the adhesive force is defined as the absolute value of the maximal normal force in the pull-off process.

3. NUMERICAL SIMULATION

Now we numerically calculate the adhesive force for different brush structures. Three types of cluster will be investigated: (1) regularly distributed pillars (Fig. 2a); (2) randomly distributed pillars (Fig. 2b); (3) mixed distribution (Fig. 2c). In case of (1), the pillars of the same sizes are placed in 4×4 (up to 32×32) lattices. In case of (2), the positions of the pillars are randomly generated in the whole square area and the circles will not overlap with each other. In the case of (3), the cubes and the pillars are mixed (the proportion is randomly given) and put into the 16×16 lattices. Their sizes in all these three distributions can also be changed to obtain various densities.

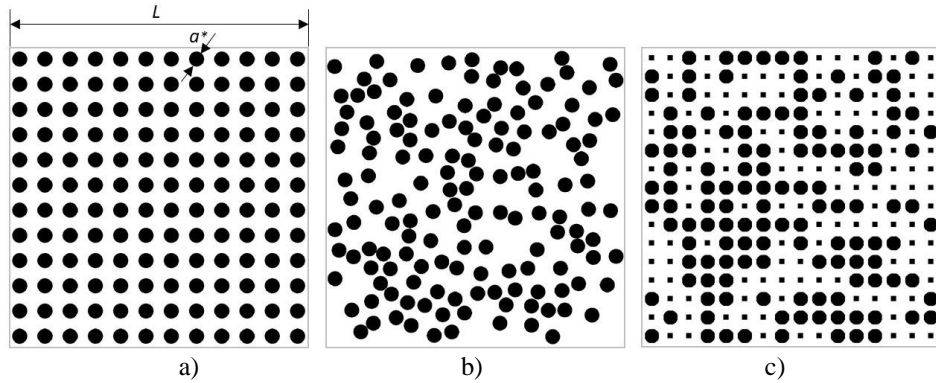


Fig. 2 Examples of three types of brush structures with $\xi = 0.29$: a) regular distribution in 12×12 lattices; b) random distribution; c) mixed distribution in 16×16 lattices

3.1. Regular distribution of pillars

In this case, the cylindrical pillars with radius a^* are regularly distributed in a square area with length L and discretization 1024×1024 . 40 densities ξ varying from 10^{-3} to 0.75 are realized through the change of radius and number of the pillars. For each ξ , we simulate the adhesion process with different numbers of pillars, from $N=4 \times 4$ to 32×32 pillars.

Fig. 3 shows an example of adhesive contact of brush with $N=16 \times 16$ pillars, where the indentation and force are normalized by the Kendall's solution for macroscopic incircle of the square area equal to Eq. (4) and (5) with $\xi=1$:

$$\bar{F}_A = \frac{F_A}{\sqrt{8\pi E^* \gamma_{12} (L/2)^3}}, \quad (6)$$

$$\bar{d} = \frac{d}{\sqrt{2\pi \xi \gamma_{12} (L/2) / E^*}}. \quad (7)$$

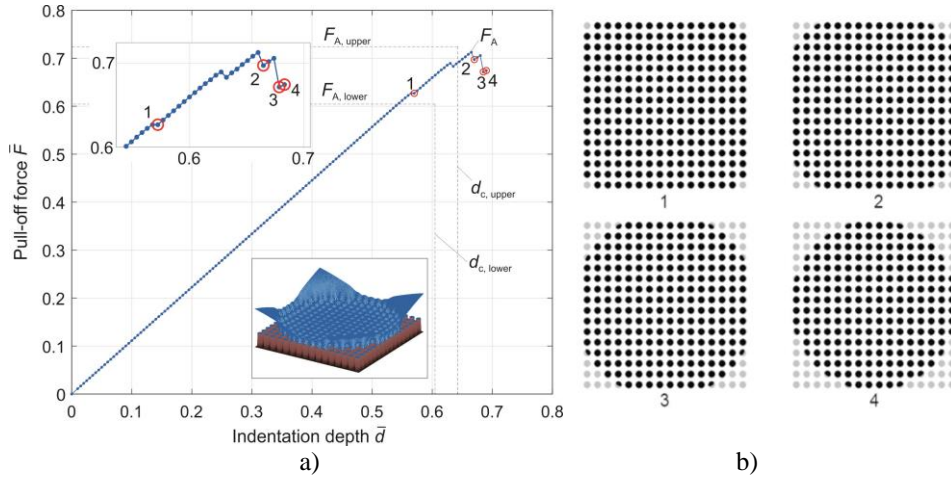


Fig. 3 Adhesive contact of a structured indenter: a) Force-indentation dependence; b) change of contact area (black color) during the detachment corresponding to the four positions in subplot (a). The gray color indicates the detached elements. The important part of the curve in subplot (a) is enlarged to observe the detachment behavior

In the simulation, the “indentation depth” is controlled during the separation and the normal force is calculated at each step. The obtained dependence of pull-off force on the separation distance is shown in Fig. 3a, where the subplot is a three-dimensional contact configuration at the final detachment moment (corresponding to point 4 in Fig. 3b). The change of contact area during the detachment can be seen in Fig.3b. It is found that the contact points at the corners are always firstly broken from the indenter and detachment expands towards the center with an increasing indentation depth. When the contact approaches the incircle of the square area, the surfaces are suddenly separated. This general

behavior has been generalized in [21] for indenters with various odd geometries. Now we put an emphasis on the maximal value of the pull-off force, i.e. adhesive force F_A . For comparison, the estimation of the upper and lower bounds of adhesive force, Eqs. (2)-(5) are also added in Fig. 3a.

Numerical results from simulations of a number of surfaces are shown in Fig. 4. For a certain area density ξ , adhesive force F_A is almost the same for different structures with few (4×4) or many (32×32) pillars (Fig. 4a). The adhesive force is roughly proportional to the square root of the contact area density (Fig. 4b).

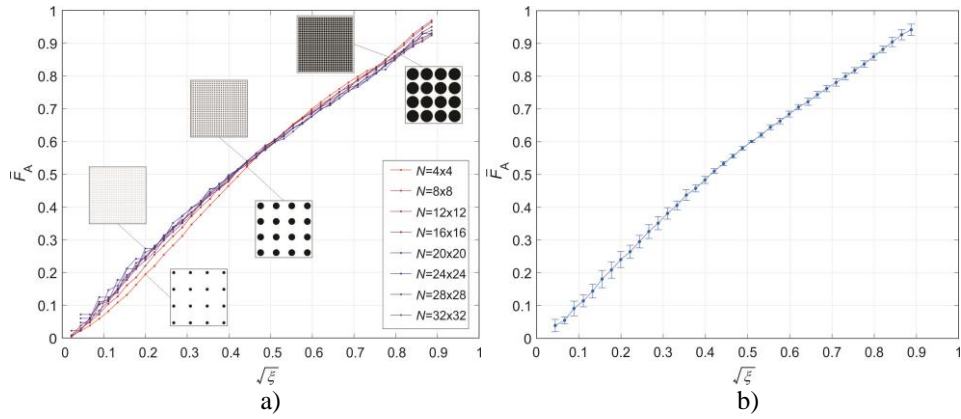


Fig. 4 Dependence of adhesive force on the square root of the filling factor: a) for different size and number of the pillars; b) in a plot with error bar

3.2. Random and mixed distribution

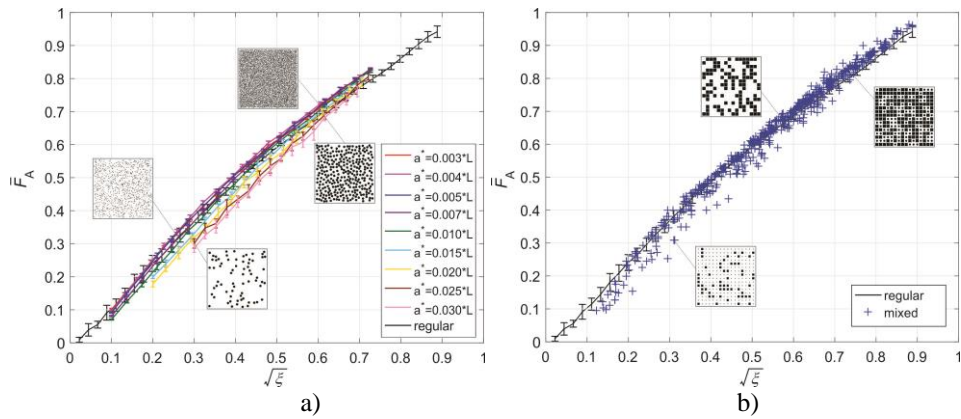


Fig. 5 Dependence of adhesive force on the square root of the filling factor: a) for randomly distributed pillars; b) for mixed distribution of pillars and squares. The adhesive force is roughly proportional to the square root of the filling factor

We have investigated other structures as shown in Fig. 2b and Fig. 2c. For the case of randomly distributed pillars, the radius of pillar a^* varies from $a^*=0.003L$ to $a^*=0.03L$. For a given radius a^* and area density ξ , the adhesive force is averaged by 10 surfaces. The results are shown in Fig. 5a, where a few examples of structure geometries are presented. The adhesive force is very slightly dependent on the size of the pillars. It is a little bit larger for smaller circles. Fig. 5b shows the results of the case for mixed distribution where the pillars and squares appear randomly on the surface. The force-area density dependence in these two cases is the same as in the case of regular distribution of pillars. For comparison, the curve of Fig. 4b for the case of regularly distributed pillars is also plotted in Figs. 5a and 5b.

4. COMPARISON WITH CIRCULAR AREA

In Fig. 3b it is seen that the detachment begins at the corner of the square and then extends toward the center. In the final state of absolute instability (complete detachment), the contact shape is approximately the incircle of the square. Numerically we simulate the pull-off adhesive contact of the same structure but macroscopically in a circular area with regularly distributed pillars. One example of force-distance relation is shown in Fig. 6a. We can see that the pull-off force increases linearly with the separation distance, and the whole circular area is found to be suddenly separated without partial detachment. This behavior is the same as in the case of a complete cylindrical punch studied by Kendall. The maximal normal force, i.e. adhesive force can be observed to be smaller than the case of square area with the same area density. The results for varied sizes of pillars presented in Fig. 6b give a similar dependence of adhesive force on the area density to the case of square area; however, in comparison with the latter, the adhesive force in the case of circular area is a little bit smaller due to a smaller contact area.

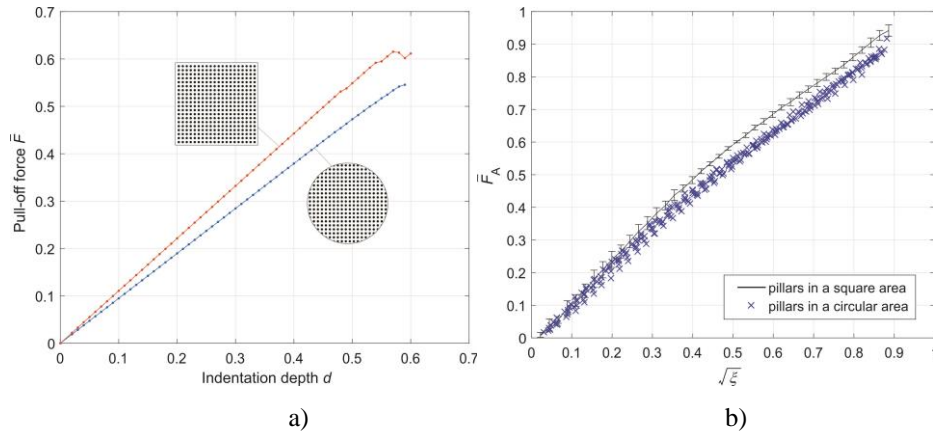


Fig. 6 Adhesive force of the pillar structure in a circular area: a) an example of force-separation dependence; b) dependence of adhesive force on the area density. The adhesive force in the case of circular area is smaller than in the case of square area

5. CONCLUSION

In this paper we have numerically simulated the pull-off adhesive contact of surfaces with brush-structures. The pillars are regularly or randomly distributed in a macroscopic square area. It is noted that we consider a rigid brush structure contacting with an elastic half space. For the case of flexible pillars, e.g. mushroom shaped microstructures [22], the behavior of detachment could be very different. As found in Ref. [21], the discontinuities of the indenter have no essential influence on the development of the detachment process: the detachment starts at the corner and spreads to the center. The adhesive force defined as the maximal pull-off force is found to be roughly proportional to the filling factor that is the ratio of pillar area and the apparent area, which verified the theoretical prediction. Therefore, the contact splitting in the case of rigid pillars does not lead to any increase in the adhesive force.

Acknowledgements: *We acknowledge financial support of the Deutsche Forschungsgemeinschaft (PO 810-55-1).*

REFERENCES

1. Checco, A., Rahman, A., Black, C.T., 2014, *Robust superhydrophobicity in large-area nanostructured surfaces defined by block-copolymer self-assembly*, Adv. Mater., 26(6), pp. 886–891.
2. Jaggessar, A., Shahali, H., Mathew, A., Yarlagadda, P.K.D.V., 2017, *Bio-mimicking nano and micro-structured surface fabrication for antibacterial properties in medical implants*, J. Nanobiotechnology, 15, pp. 1–20.
3. D. Gropper, D., Wang, L., Harvey, T.J., 2016, *Hydrodynamic lubrication of textured surfaces: A review of modeling techniques and key findings*, Tribol. Int., 94, pp. 509–529.
4. Autumn, K., 2002, *Mechanisms of Adhesion in Geckos*, Integr. Comp. Biol., 42(6), pp. 1081–1090.
5. Arzt, E., Gorb, S., Spolenak, R., 2003, *From micro to nano contacts in biological attachment devices*, Proc. Natl. Acad. Sci., 100(19), pp. 10603–10606.
6. Kamperman, M., Kroner, E., del Campo, A., McMeeking, R.M., Arzt, E., 2010, *Functional adhesive surfaces with “gecko” effect: The concept of contact splitting*, Adv. Eng. Mater., 12, pp. 335–348.
7. Popov, V.L., 2017, *Contact Mechanics and Friction, 2nd Edition*, Springer Verlag.
8. Kendall, K., 1971, *The adhesion and surface energy of elastic solids*, J. Phys. D: Appl. Phys., 4, pp. 1186–1195.
9. Guidoni, G.M., Schillo, D., Hangen, U., Castellanos, G., Arzt, E., McMeeking, R.M., Bennewitz, R., 2010, *Discrete contact mechanics of a fibrillar surface with backing layer interactions*, J. Mech. Phys. Solids., 58, pp. 1571–1581.
10. Argatov, I.I., 2011, *Electrical contact resistance, thermal contact conductance and elastic incremental stiffness for a cluster of microcontacts: Asymptotic modelling*, Quart. J. Mech. Appl. Math., 64, pp. 1–24.
11. Bacca, M., Booth, J.A., Turner, K.L., McMeeking, R.M., 2016, *Load sharing in bioinspired fibrillar adhesives with backing layer interactions and interfacial misalignment*, J. Mech. Phys. Solids, 96, pp. 428–444.
12. Argatov, I.I., Li, Q., Popov, V.L., 2018, *Cluster of the Kendall-type adhesive microcontacts as a simple model for load sharing in bioinspired fibrillar adhesives*, submitted.
13. Pohrt, R., Popov, V.L., 2015, *Adhesive contact simulation of elastic solids using local mesh-dependent detachment criterion in boundary elements method*, Facta Univ. Ser. Mech. Eng., 13(1), pp. 3–10.
14. Bazrafshan, M., de Rooij, M.B., Valefi, M., Schipper, D.J., 2017, *Numerical method for the adhesive normal contact analysis based on a Dugdale approximation*, Tribol. Int., 112, pp. 117–128.
15. Rey, V., Anciaux, G., Molinari, J.F., 2017, *Normal adhesive contact on rough surfaces: efficient algorithm for FFT-based BEM resolution*, Comput. Mech., 60, pp. 69–81.
16. Johnson, K.L., Kendall, K., Roberts, A.D., 1971, *Surface energy and the contact of elastic solids*, Proc. R. Soc. A, 324, pp. 301–313.
17. Argatov, I.I., Li, Q., Pohrt, R., Popov, V.L., 2016, *Johnson-Kendall-Roberts adhesive contact for a toroidal indenter*, Proc. R. Soc. London A Math. Phys. Eng. Sci., 472.

18. Li, Q., Argatov, I.I., Popov, V.L., 2018, *Onset of detachment in adhesive contact of an elastic half-space and flat-ended punches with noncircular shape: Analytic estimations and comparison with numeric analysis*, submitted.
19. Li, Q., Popov, V.L., 2017, *Boundary element method for normal non-adhesive and adhesive contacts of power-law graded elastic materials*, *Comput. Mech.*, doi: doi: 10.1007/s00466-017-1461-9.
20. Heß, M., 2016, *A simple method for solving adhesive and non-adhesive axisymmetric contact problems of elastically graded materials*, *Int. J. Eng. Sci.*, 104, pp. 20–33.
21. Popov, V.L., Pohrt, R., Li, Q., 2017, *Strength of adhesive contacts: Influence of contact geometry and material gradients*, *Friction*, 5, pp. 308–325.
22. Heepe, L., Gorb, S.N., 2014, *Biologically Inspired Mushroom-Shaped Adhesive Microstructures*, *Annu. Rev. Mater. Res.*, 44, pp. 173–203.